ACS Catalysis

Research Article

pubs.acs.org/acscatalysis

Comparative Study on the Sulfur Tolerance and Carbon Resistance of Supported Noble Metal Catalysts in Steam Reforming of Liquid Hydrocarbon Fuel

Chao Xie,[†,‡] Yongsheng Chen,[†,§] Mark H. Engelhard,[⊥] and Chunshan Song*[,†,§]

[†]Clean Fuels and Catalysis Program, EMS Energy Institute, The Pennsylvania State University, 209 Academic Projects Building, University Park, Pennsylvania 16802, United States

[‡]Department of Materials Science and Engineering and [§]Department of Energy and Mineral Engineering, The Pennsylvania State University, University Park, Pennsylvania 16802, United States

[⊥]Environmental Molecular Sciences Laboratory, Pacific Northwest National Laboratory, Richland, Washington 99352, United States

ABSTRACT: This work was conducted to clarify the influence of the type of metal and support on the sulfur tolerance and carbon resistance of supported noble metal catalysts in steam reforming of liquid hydrocarbons. Al_2O_3-supported noble metal catalysts (Rh, Ru, Pt, and Pd), Rh catalysts on different supports (Al_2O_3, CeO_2, SiO_2, and MgO), and Pt catalysts supported on CeO_2 and Al_2O_3, were examined for steam reforming of a liquid hydrocarbon fuel (Norpar13 from Exxon Mobil) at 800 °C for 55 h. The results indicate that (1) Rh/Al_2O_3 shows higher sulfur tolerance than the Ru, Pt, and Pd catalysts on the same support; (2) both Al_2O_3 and CeO_2 are promising supports for Rh catalyst to process sulfur-containing hydrocarbons; and (3) Pt/CeO_2 exhibits better catalytic performance than Pt/Al_2O_3 in the reaction with sulfur. Transmission electron microscopy (TEM) results demonstrate that the metal particles in Rh/Al_2O_3 were better dispersed (mostly in 1−3 nm) compared with the other catalysts after reforming the sulfur-containing feed. As revealed by X-ray photoelectron spectroscopy (XPS), the binding energy of Rh 3d for Rh/Al_2O_3 is notably higher than that for Rh/CeO_2, implying the formation of electron-deficient Rh particles in the former. The strong sulfur tolerance of Rh/Al_2O_3 may be related to the formation of well-dispersed electron-deficient Rh particles on the Al_2O_3 support. Sulfur K-edge X-ray absorption near edge structure (XANES) spectroscopy illustrates the preferential formation of sulfonate and sulfate on Rh/Al_2O_3, which may be beneficial for improving its sulfur tolerance as their oxygen-shielded sulfur structure may hinder direct Rh−S interaction. Because of its strong sulfur tolerance, the carbon deposition on Rh/Al_2O_3 was significantly lower than that on the Al_2O_3-supported Ru, Pt, and Pd catalysts after the reaction with sulfur. The superior catalytic performance of CeO_2-supported Rh and Pt catalysts in the presence of sulfur can be ascribed mainly to the promotion effect of CeO_2 on carbon gasification, leading to much lower carbon deposition compared with that for the Rh/Al_2O_3, Rh/MgO, Rh/SiO_2, and Pt/Al_2O_3 catalysts.

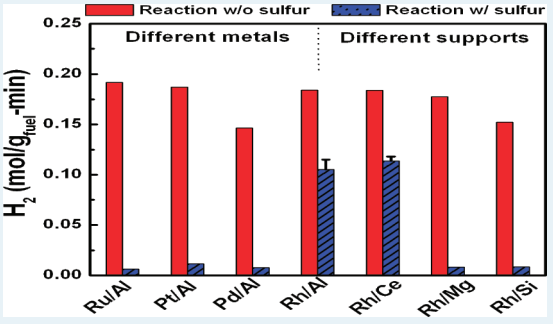

KEYWORDS: *noble metal catalyst, sulfur poisoning, carbon deposition, hydrocarbon reforming, deactivation, hydrogen, XANES*

1. INTRODUCTION

Steam reforming of liquid hydrocarbon fuels is expected to play an important role in hydrogen production for on-site and on-board fuel cell applications.[1] Ni catalysts are extensively used in the steam reforming process mainly because of their cost-effective and widely available characteristics. However, they are prone to carbon deposition, which is very deleterious to hydrocarbon reforming reactions over their surfaces.[1−15] For example, numerous studies have pointed out that filamental carbon can readily form on Ni catalysts to cause their deactivation and plug reforming reactors.[5−8,16−19] In this aspect, carbon-resistant noble metal catalysts such as Rh, Ru, Pt, and Pd are more attractive.[2,6,7,16] In general, the kinetics of carbon gasification on noble metals is fast, and the growth of filamental carbon on them is unfavorable because of the low carbon solubility in their bulk. Moreover, liquid hydrocarbon fuels (e.g., gasoline, diesel, and jet fuel) usually contain sulfur impurities that can poison reforming catalysts as a result of strong chemisorptive sulfur adsorption on metals.[3,19−21] Therefore, catalyst deactivation because of sulfur poisoning has been recognized as a major challenge for the practical applications of liquid hydrocarbon reforming technology.[1,22,23] Some previous studies reported that noble metal catalysts possess better sulfur tolerance than Ni.[22,24−29] For example, Lu et al. developed a $Pt/Ce_{0.8}Gd_{0.2}O_{1.9}$ catalyst, which is more sulfur tolerant compared with a Ni catalyst on the same support in steam reforming of iso-octane with sulfur at 800 °C.[28,29] Our recent work[22,30] demonstrated that deactivation of a $Ni/CeO_2−Al_2O_3$ catalyst was much more severe than that of a $Rh/CeO_2−Al_2O_3$

Received: December 30, 2011
Revised: March 6, 2012
Published: April 18, 2012

catalyst in steam reforming of liquid hydrocarbons with sulfur at 800 °C. We employed carbon K-edge X-ray absorption near edge structure (XANES) spectroscopy to comparatively study the influence of sulfur on the carbon deposition on the Ni and Rh catalysts during steam reforming of liquid hydrocarbons.[31] It was illustrated that the presence of sulfur increased the carbon deposition on both catalysts, which has a much more significant impact for the Ni catalyst. Carbon K-edge XANES study on the used catalysts revealed that graphitic carbon was dominant in the presence of sulfur, while oxidized carbon species (quinone-like carbon, carboxyl, and carbonate) prevailed without sulfur. Meanwhile, the formation of carboxyl and carbonate more dramatically dropped on the Ni catalyst than that on the Rh catalyst. In view of these results, we could infer that (I) the presence of sulfur can suppress carbon gasification and lead to the enhanced formation of graphitic carbon on reforming catalysts in liquid hydrocarbon reforming, and (II) Rh catalyst possesses stronger capability to maintain carbon gasification activity than Ni catalyst in the presence of sulfur. Owing to their promising resistance to carbon deposition and potential sulfur tolerance, supported noble metal catalysts are being widely studied in the field of hydrocarbon processing for the production of clean fuels such as H_2.[24,25,28,29,32−34]

In the present study, a variety of noble metal catalysts including Al_2O_3-supported noble metals (Rh, Ru, Pt, and Pd), Rh catalysts on different supports (Al_2O_3, CeO_2, SiO_2, and MgO), and Pt catalyst supported on CeO_2 were prepared and examined for steam reforming of liquid hydrocarbon fuel in the absence and presence of sulfur at 800 °C. The goal of this work is to clarify the influence of the type of metal and support on the sulfur tolerance and carbon resistance of supported noble metal catalysts in steam reforming of sulfur-containing liquid hydrocarbon fuel. In addition to characterization of the fresh catalysts using H_2-TPR, and H_2-chemisorption, high-resolution transmission electron microscopy (TEM) and sulfur K-edge XANES spectroscopy were employed to characterize the metal particle sizes and to identify the sulfur species in the used catalysts after the reforming reactions with sulfur.

2. EXPERIMENTAL SECTION

2.1. Catalyst Preparation. High-purity reagent-grade $Rh(NO_3)_3$ (Aldrich), $RuCl_3$ (Aldrich), $PtCl_4$ (Pressure Chemical Co.), $Pd(NO_3)_2$ (Aldrich), $Ce(NO_3)_3$ (Alfa Aesar), $Mg(NO_3)_2$ (Aldrich), and SiO_2 (Aldrich) were used as received. The noble metal catalysts (Rh, Ru, Pt, and Pd) supported on Al_2O_3 were prepared by wet impregnation of the corresponding metal salts onto the Al_2O_3 support (Sasol PURALOX TH 100/150) at 2 wt % of metal loading. The CeO_2 and MgO supports were prepared by calcination of $Ce(NO_3)_3$ and $Mg(NO_3)_2$ at 550 °C for 6 h, respectively. The Rh (2 wt %) catalysts supported on SiO_2, CeO_2, and MgO as well as Pt (2 wt %) catalyst supported on CeO_2 were prepared using the same approach as above-mentioned. All the catalysts were calcined at 550 °C for 6 h.

2.2. Catalytic Reactions. Approximately 1 g of catalyst with particle sizes of 18−35 mesh (0.5−1 mm) was placed in the center of a stainless steel tube (0.54 in. o.d., 0.375 in. i.d., 24 in. long) with the rest of the tube being packed with α-alumina beads. The reforming reactions were performed at 800 °C. Prior to the reactions, the catalysts were reduced by pure hydrogen at 800 °C. Both water and fuel were pumped via HPLC pumps through a preheater and then into the reactor at volumetric flow rates of 4.08 and 1.38 mL/h, respectively, for a steam-to-carbon molar ratio (S/C) of 3:1 and feed weight hourly space velocity (WHSV) of 5.1 h^{-1}. The fuel employed in this study was sulfur-free Norpar13, a liquid hydrocarbon fuel (Exxon Mobil) composed of normal paraffins (>99%) with an average carbon number of 13. The experiments with sulfur were carried out by doping Norpar13 with 3-methylbenzothiophene (3-MBT) for an equivalent 350 ppmw (parts per million by weight) of sulfur. In the present work, the catalyst performances were compared on equal mass basis (i.e., 1 g of supported metal catalysts containing 2 wt % of noble metal loading). As shown in our previous study,[30] control experiments illustrated that, in the absence of reforming catalyst, the liquid hydrocarbon fuel is completely decomposed to gas-phase smaller hydrocarbon molecules (e.g., C1−C4 hydrocarbons) at 800 °C in a stainless steel reactor, but with negligible hydrogen formation. Therefore, hydrogen production rate (HPR), which is defined as (moles of H_2 produced per minute)/(grams of hydrocarbon fed), was used in the present study to evaluate the catalyst performance. After the control experiments, little carbon deposition was formed on the stainless steel reactor by visual inspection, suggesting that the reactor barely affected the carbon deposition in the reforming reactions. For all the catalysts in the sulfur-free reactions, the HPRs were stable during 55 h on steam (i.e., the initial HPR was basically the same as that at the end of reaction), and no sign of catalyst deactivation was observed. For the sulfur-containing reactions, the initial HPR was almost the same as that in the absence of sulfur for a given catalyst. However, because of catalyst deactivation in the presence of sulfur, the HPR rapidly dropped with time on steam for all the catalysts except the Rh catalysts supported on Al_2O_3 and CeO_2. The percentage of activity loss was used to evaluate the sulfur tolerance and carbon resistance of the noble metal catalysts in the reactions with sulfur-containing feed. The percentage of activity loss = [HPR(w/o S) − HPR (w/S)] × 100/[HPR(w/o S)], where HPR(w/oS) and HPR(w/S) stand for the HPR in the absence and presence of sulfur for a given catalyst, respectively. The HPRs used in this equation were measured after 55 h on stream. The percentage of activity loss indicates the activity loss for a given catalyst in steam reforming of sulfur-containing feed compared with the corresponding sulfur-free case.

2.3. Catalyst Characterization. The physicochemical properties of the fresh catalysts were characterized by the BET (Brunauer−Emmett−Teller) method, H_2 temperature-programmed reduction (H_2-TPR), and H_2-chemisorption. BET measurements were carried out at liquid N_2 temperature (−196 °C) with a Quartchrome Autosorb-1 analyzer. Each sample was degassed by heating at 200 °C under vacuum prior to the BET analysis. H_2-TPR was conducted on a Micromeritics AutoChem 2910 with 5% H_2 in Ar at a temperature ramp of 5 °C/min. H_2 chemisorption was conducted using the same device to measure the metal dispersion of the fresh catalysts. The sample was reduced in hydrogen at 500 °C, followed by cooling down to 50 °C under Ar, then pulsing with 24.3% H_2 in Ar at 50 °C until saturation. To minimize the impact of ceria reduction on the H_2 chemisorption on ceria-supported catalysts,[35,36] the Rh/CeO_2 and Pt/CeO_2 catalysts were reduced at 150 °C prior to the H_2 chemisorption experiment, as reported by Kugai et al.[37] Literature[38] has illustrated that ceria reduction in CeO_2-supported noble metal catalysts becomes significant at temperatures higher than 200 °C because of the rapid hydrogen spillover from reduced noble metals to adjacent ceria thus facilitating the reduction of the latter. Because of the pronounced effect of reduced ceria on H_2 chemisorption, the reduction temperature for Rh/CeO_2 and Pt/CeO_2 was fixed at 150 °C. The metal dispersion was calculated by assuming an adsorption stoichiometry of one H atom per surface metal atom.[23,39] The results of BET and H_2 chemisorption are summarized in Table 1.

dx.doi.org/10.1021/cs200695t | ACS Catal. 2012, 2, 1127−1137

Table 1. Physical Properties of the Noble Metal Catalysts Studied in This Work

catalysts	S_{BET} (m^2/g_{cat})	pore vol. (cm^3/g)	dispersion (%)	metal particle size (nm) H/M[a]	metal particle size (nm) TEM/STEM[b]
Rh/Al_2O_3	148.3	0.77	49.3	2.0	1–3
Rh/CeO_2	92.9	0.18	45.6	2.2	5–7
Pt/Al_2O_3	137.8	0.81	53.4	1.9	8–13
Pt/CeO_2	83.2	0.13	30.2	3.3	6–12
Ru/Al_2O_3	136.1	0.76	6.1	16.3	10–18
Pd/Al_2O_3	134.3	0.69	6.9	14.5	17–25
Rh/SiO_2	378.6	0.29	48.6	2.0	9–18
Rh/MgO	36.7	0.08	35.4	2.8	3–14

[a]Based on the H_2 chemisorption on the fresh noble metal catalysts. The metal particle size (d) was calculated from the equation d = 1/dispersion (nm) [39] [b]Based on the TEM/STEM characterization results of the used noble metal catalysts after Norpar13(350) reforming at 800 °C for 55 h, as shown in Figures 4 and 10.

X-ray photoelectron spectroscopy (XPS) measurements of the unreduced and reduced Rh catalysts supported on Al_2O_3 and CeO_2 were performed on a Physical Electronics Quantum 2000 Scanning ESCA microprobe located at Environmental Molecular Sciences Laboratory in the Pacific Northwest National Laboratory. The fresh catalyst was loaded in a quartz reactor and reduced under a 10% H_2/He mixture (100 mL/min in total) at 800 °C for 1 h before cooling down to room temperature. The quartz reactor is connected to the XPS analytical chamber such that the reduced sample can be transferred into the chamber without air exposure. The XPS instrument uses a focused monochromatic Al Kα X-ray (1486.7 eV) source for excitation and a spherical section analyzer. The X-ray beam used is a 105-W, 100-μm X-ray beam spot rastered on the sample. Electrons of 1 eV, 20 μA, and low-energy Ar^+ ions were used to avoid the charging on the catalysts during XPS analysis. The binding energy values were referenced using 916.7 (Ce $3d_{3/2}$ $4f_0$) and 74.7 eV (Al 2p) for the Rh/CeO_2 and Rh/Al_2O_3 catalysts, respectively.

The carbon and sulfur contents in used catalysts after the reaction with sulfur were determined by a LECO SC 144DR analyzer. The sample was burnt in a pure oxygen environment at 1350 °C, allowing the carbon and sulfur species to be converted to CO_2 and SO_2, respectively. An IR cell was used to measure the concentration of CO_2 and SO_2, from which the carbon and sulfur contents on the used catalysts were determined. High-resolution TEM images of the used catalysts upon the reaction with sulfur were recorded by JEOL 2010F at 200 kV accelerating voltage. Their Z-contrast images were obtained on the same instrument using the scanning transmission electron microscope (STEM) mode. Since the Z-contrast images are directly related to the atomic numbers of materials studied, it is feasible to distinguish the metals from supports for our used reforming catalysts. For example, in the cases of Al_2O_3 supported Rh, Ru, Pt, and Pd catalysts, the noble metals appear to be much brighter than the Al_2O_3 support because of their heavier characteristics (higher atomic numbers). In a typical TEM sample preparation, the used catalyst was dispersed in ethanol with the aid of sonication, and several drops of the suspension were deposited on a copper grid. Sulfur K-edge XANES measurements of the used catalysts after the reaction with sulfur were performed at Beamline 9-BM-B of the Advanced Photon Source (APS) at Argonne National Laboratory. The storage ring was operated with an electron beam of 7 GeV and an electron current of 100 mA in a top-up mode. The monochromator was double-crystal Si(111), and the XANES spectra were collected in fluorescence mode with a Si DRIFT 4-element detector (Vortex). Air absorption was controlled by the use of helium purging in the incident light path and the sample chamber, which were separated by a 5 μm thick polycarbonate window. The monochromator crystals were Si(111) with an energy resolution of approximately 0.3 eV at 2.5 keV. Harmonics were rejected by use of a Rh-coated flat mirror in the experimental station. The beam was focused to a spot size of approximately 1 mm in the horizontal and vertical directions by the use of a Rh-coated toroidal mirror. A small amount of well-ground sample was evenly spread over a sulfur-free tape. Energy calibration was accomplished by setting the edge energy of elemental sulfur to 2472.0 eV. All the XANES data were processed using Athena.[40]

3. RESULTS

3.1. Al_2O_3-Supported Noble Metal Catalysts. The hydrogen production rates (HPR) for the Al_2O_3-supported noble metal catalysts (Rh, Ru, Pt, and Pd) upon reforming of Norpar13 and Norpar13 doped with 350 ppmw sulfur (referred to as Norpar13(350)) for 55 h are exhibited in Figure 1. For the sulfur-free cases, the HPRs for the Rh, Ru, and Pt catalysts were comparable, and slightly higher than that of Pd. Although the presence of sulfur deactivated all the Al_2O_3-supported noble metal catalysts in Norpar13(350) reforming to some extent, the activity loss for Rh/Al_2O_3 was the lowest (44, 96, 94, and 95% for the activity losses for the Rh, Ru, Pt, and Pd catalysts, respectively) (see Figure 1). This fact implies that Rh/Al_2O_3 possesses stronger sulfur tolerance than the other Al_2O_3-supported noble metals in steam reforming of Norpar13 with 350 ppmw sulfur at 800 °C.

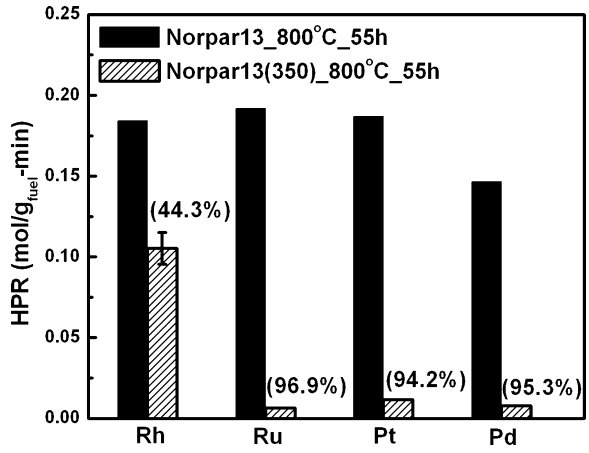

Figure 1. Catalytic performances of Al_2O_3-supported Rh, Ru, Pd, and Pt catalysts in steam reforming of Norpar13 and Norpar13 doped with 350 ppmw sulfur (Norpar13(350)) at 800 °C after 55 h on stream. The catalyst performances were compared on equal mass basis (i.e., 1 g of each supported metal catalyst was used, which contained 2 wt % of noble metal). The number in the parentheses represents the percentage of activity loss for the catalysts in the reaction with sulfur compared with the sulfur-free reaction after 55 h on stream. The percentage of activity loss was defined in the Experimental Section.

The carbon amounts in the used Al_2O_3-supported noble metal catalysts after the reactions without and with sulfur for

dx.doi.org/10.1021/cs200695t | ACS Catal. 2012, 2, 1127–1137

55 h are presented in Figure 2. Compared with the sulfur-free reaction, the carbon deposition dramatically increased upon Norpar13(350) reforming, which is especially significant for the Ru, Pt, and Pd catalysts. Figure 3 exhibits the sulfur contents in

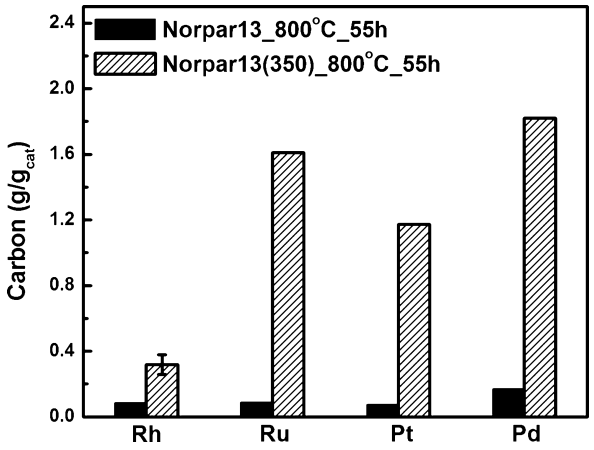

Figure 2. Carbon contents in the used Al_2O_3-supported Rh, Ru, Pd, and Pt catalysts after steam reforming of Norpar13 and Norpar13 doped with 350 ppmw sulfur (Norpar13(350)) at 800 °C after 55 h on stream.

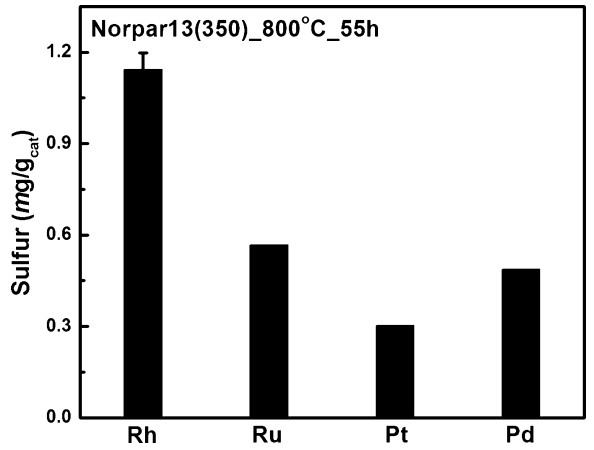

Figure 3. Sulfur contents in the used Al_2O_3-supported Rh, Ru, Pd, and Pt catalysts after steam reforming of Norpar13 doped with 350 ppmw sulfur (Norpar13(350)) at 800 °C after 55 h on stream.

the used Al_2O_3-supported noble metal catalysts after Norpar13(350) reforming for 55 h. It is worth noting that, as shown in Figure 3, the sulfur content in the used Rh/Al_2O_3 is about 2−3 times higher than those in the used Ru, Pt, and Pd catalysts, though its catalytic performance is the best among all the Al_2O_3-supported noble metal catalysts in the case of Norpar13(350) reforming.

Figure 4 presents the TEM and *Z*-contrast (STEM) images of the used Al_2O_3-supported Rh, Ru, Pt, and Pd catalysts upon Norpar13(350) reforming for 55 h. It is apparent that the Rh particles are well dispersed on Al_2O_3 in the range of 1−3 nm. This observation is consistent with previous studies demonstrating that Rh tends to homogeneously distribute on Al_2O_3.[41−43] Beck et al.[44] used EXAFS to characterize a Rh catalyst supported on Al_2O_3, and demonstrated that the Rh particles in this catalyst were in the range of 1−2 nm. It was proposed that rhodium atoms in Rh/Al_2O_3 can strongly interact with the oxygen ions in the Al_2O_3 support, which is capable of effectively stabilizing Rh particles against metal sintering.[41,42] In contrast, much larger metal particles in the range of 10−25 nm can be clearly seen in the other Al_2O_3-supported noble metal catalysts (Ru, Pt, and Pd). Apparently, the dispersion of other noble metals on Al_2O_3 was lower compared with Rh/Al_2O_3, which is consistent with previous studies.[32,33,41,44−46] For example, Nagai et al. showed that the Pt particles in a Pt/Al_2O_3 catalyst were mostly larger than 10 nm after 800 °C aging in air for 5 h.[46] Zhao et al. reported that the Ru particle sizes of Ru/Al_2O_3 upon calcination at 500 °C were between 10 and 15 nm.[45]

To gain insight into the dramatically different sulfur tolerance of the Al_2O_3-supported Rh, Ru, Pt, and Pd catalysts, sulfur K-edge XANES was carried out to identify the sulfur species in these used catalysts after Norpar13(350) reforming for 55 h, as shown in Figure 5. With respect to the Rh/Al_2O_3 catalyst, four sulfur species are observed, which are metal sulfide (Rh−S) at 2472 eV, organic sulfide (-C-S-C-) at 2475 eV, sulfonate (C_xH_y-SO_2O^-) at 2481 eV, and sulfate (SO_4^{2-}) at 2483 eV.[47,48] Although the same sulfur species are detected with the other used Al_2O_3-supported noble metal catalysts, their relative abundances are dramatically different from that of Rh/Al_2O_3. The Ru, Pt, and Pd catalysts show strong peaks of organic sulfides, but with notably weaker peaks of metal sulfide, sulfonate, and sulfate. We believe that the organic sulfides are largely derived from the adsorption of the organic sulfur compound (3-MBT) in the fuel and its pyrolytic deposits containing -C-S-C- onto the catalysts. It seems that the formation of organic sulfides is somehow correlated with the abundant carbon deposits. This may be because the carbon species can cover reforming catalysts to hinder the desorption of organic sulfides. Moreover, the excessive carbon deposits may cover the metal surfaces of the Ru, Pt, and Pd catalysts so as to suppress sulfur adsorption on the metals as well as the formation of the oxidized sulfur species. These postulations may explain the weak peaks of metal sulfide, sulfonate, and sulfate in the sulfur XANES spectra of the used Al_2O_3-supported Ru, Pt, and Pd catalysts.

3.2. Rh and Pt Catalysts on Different Supports. Since the Rh/Al_2O_3 exhibited better sulfur tolerance than the Al_2O_3 supported Ru, Pt, and Pd catalysts under the reforming conditions used in this study, the Rh catalysts on different supports (Al_2O_3, CeO_2, SiO_2, and MgO) were further studied to evaluate the effect of support on the sulfur tolerance of Rh. In addition to Rh, Pt is another metal catalyst commonly used in liquid hydrocarbon reforming.[28,29] Therefore, the catalytic performances of Pt catalysts supported on Al_2O_3 and CeO_2 were also compared in this work. Figure 6 displays the TPR profiles for the Rh catalysts on the different supports. Rh/Al_2O_3 shows a very broad profile up to 600 °C because of the reduction of Rh_2O_3. The rhodium reduction for Rh/SiO_2 and Rh/MgO is accomplished at lower temperatures around 200 and 400 °C, respectively. Rh/CeO_2 exhibits two peaks at 150 and 200 °C as a result of the reduction of Rh_2O_3 and CeO_2, respectively.[39] Since the reduction of CeO_2 alone generally takes place at temperatures higher than 400 °C,[49] it can be inferred that the presence of Rh is able to facilitate the reduction of CeO_2. This is very likely due to the facile H_2 dissociation on Rh, followed by spillover of H species onto CeO_2.[39,49] Compared with the other Rh catalysts, the reduction peak in Rh/Al_2O_3 is much broader. This may be due to the intimate interaction between rhodium and alumina, thus making Rh reduction relatively difficult.[43,44,50]

Figure 7 presents the catalytic performances of the Rh catalysts on the different supports (Al_2O_3, CeO_2, MgO, and SiO_2) after reforming of Norpar13 and Norpar13(350) for 55 h. In the case of

dx.doi.org/10.1021/cs200695t | *ACS Catal.* 2012, 2, 1127−1137

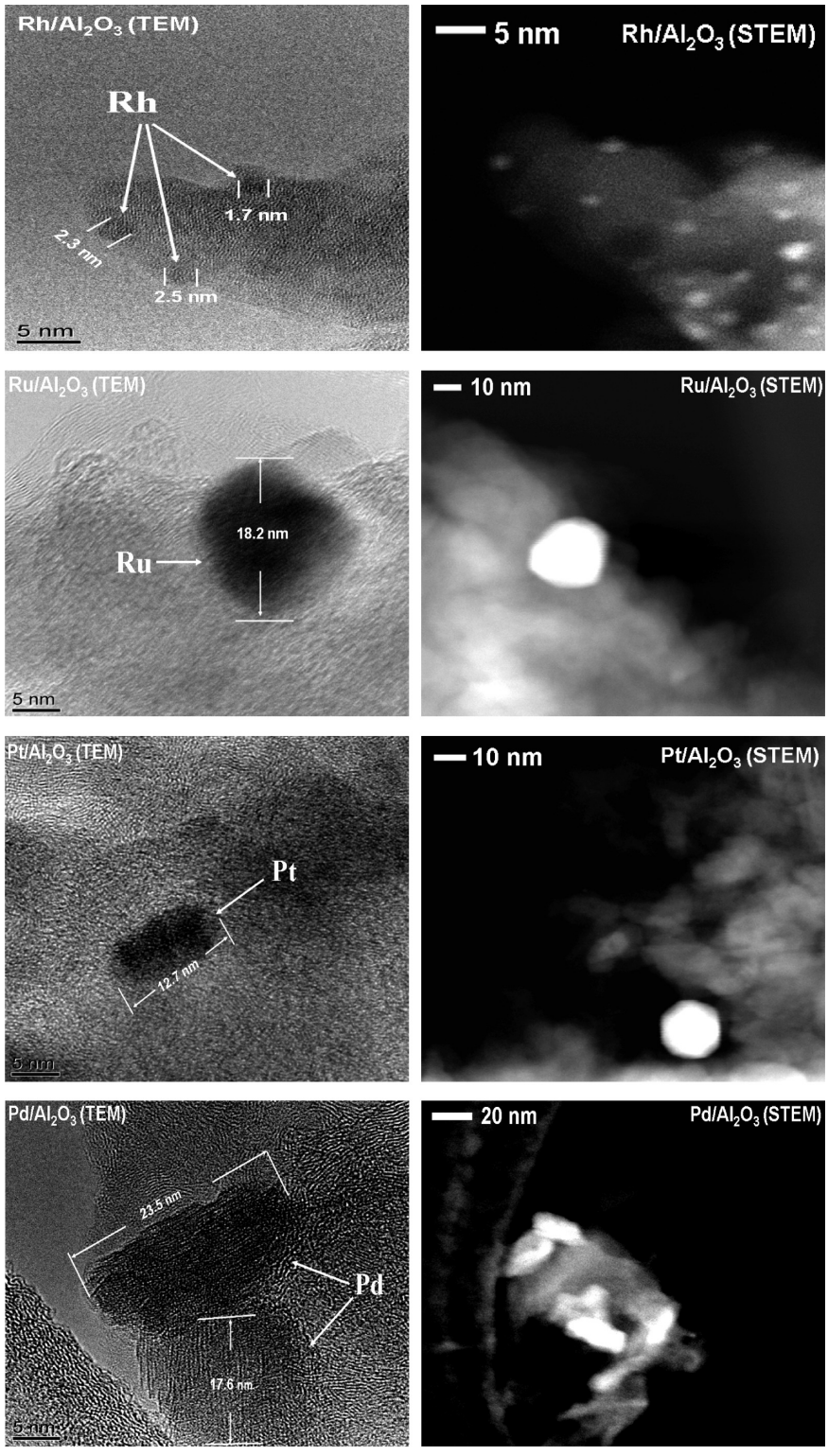

Figure 4. High-resolution TEM and *Z*-contrast (STEM) images of the used Al_2O_3-supported Rh, Ru, Pd, and Pt catalysts after steam reforming of Norpar13 doped with 350 ppmw sulfur (Norpar13(350)) at 800 °C after 55 h on stream. The brighter spots in the *Z*-contrast (STEM) images represent metal particles. The white lines in the TEM images were used to help locate the noble metal particles and measure their sizes.

Norpar13 reforming, the Rh catalysts supported on Al_2O_3, CeO_2, and MgO exhibited similar H_2 production rates, which are higher than that of Rh/SiO_2. In the presence of sulfur, both Rh/SiO_2 and Rh/MgO are significantly deactivated (the activity losses are nearly 95% for both), while the activity losses for Rh/Al_2O_3 and Rh/CeO_2 are much less (44 and 38% for Rh/Al_2O_3 and Rh/CeO_2, respectively). The significantly different catalytic performances of these Rh catalysts in Norpar13(350) reforming reflect the crucial role of support in determining the sulfur tolerance of Rh catalysts in hydrocarbon reforming.

The Pt/CeO_2 catalyst was also tested for Norpar13(350) reforming at 800 °C for 55 h on stream, and compared with

dx.doi.org/10.1021/cs200695t | *ACS Catal.* 2012, 2, 1127–1137

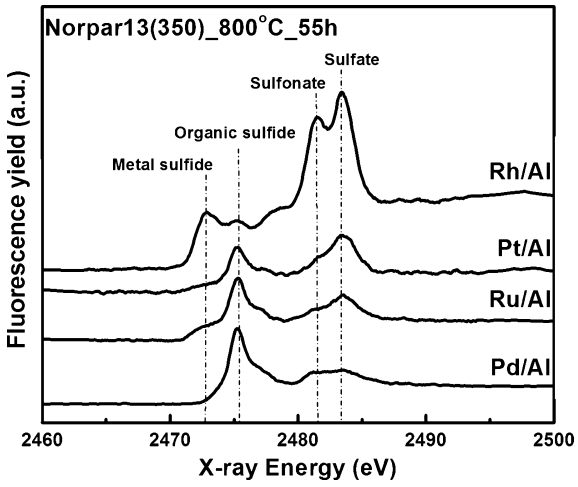

Figure 5. Sulfur K-edge XANES spectra of the used Al_2O_3-supported Rh, Ru, Pd, and Pt catalysts after steam reforming of Norpar13 doped with 350 ppmw sulfur (Norpar13(350)) at 800 °C after 55 h on stream.

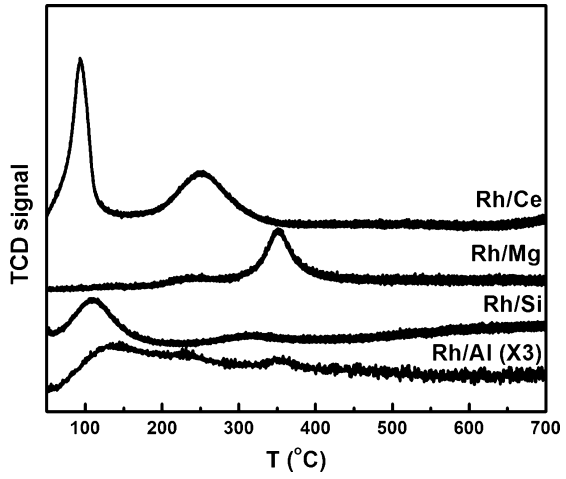

Figure 6. H_2-TPR profiles of the fresh Rh catalysts supported on Al_2O_3, CeO_2, SiO_2, and MgO.

Pt/Al_2O_3 in the same reaction. Apparently, the H_2 production with the Pt/CeO_2 catalyst (0.06 mol/g_{fuel}-min) was much more effective than that with the Pt/Al_2O_3 catalyst (0.01 mol/g_{fuel}-min) in the presence of sulfur. This further confirms that CeO_2 is a good support for noble metal catalysts to reform sulfur-containing liquid hydrocarbons, which is in good agreement with previous work.[29]

The carbon amounts on the used Rh catalysts after reforming of Norpar13 and Norpar13(350) for 55 h as well as that on the used Pt/CeO_2 catalyst after Norpar13(350) reforming for 55 h are compared in Figure 8. In the absence of sulfur, the carbon deposition on Rh/SiO_2 is much more severe than that on the other Rh catalysts. The excessive carbon deposits on Rh/SiO_2 may account for its deactivation in reforming of Norpar13. Evidently, the carbon amounts for the used Rh catalysts after Norpar13(350) reforming are higher than those after Norpar13 reforming, which is also true for the Al_2O_3-supported noble metal catalysts (Figure 2). It is therefore clear that the presence of sulfur can enhance the carbon deposition on reforming catalysts, which is consistent with our previous study.[31] The amounts of carbon deposits on the used CeO_2-supported Rh and Pt are remarkably

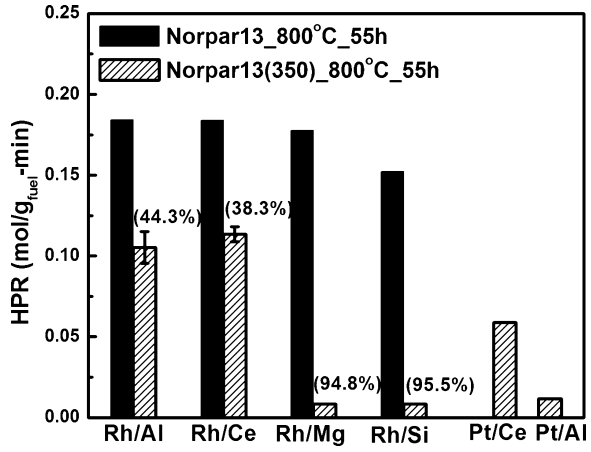

Figure 7. Catalytic performances of the Rh catalysts supported on Al_2O_3, CeO_2, SiO_2, and MgO in steam reforming of Norpar13 and Norpar13 doped with 350 ppmw sulfur (Norpar13(350)) as well as the Pt/CeO_2 and Pt/Al_2O_3 catalysts in steam reforming of Norpar13(350) at 800 °C after 55 h on stream. The catalyst performances were compared on equal mass basis (i.e., 1 g of supported metal catalyst containing 2 wt % of noble metal loading). The number in the parentheses represents the percentage of activity loss for the catalysts in the reaction with sulfur compared with the sulfur-free reaction after 55 h on stream. The percentage of activity loss was defined in the Experimental Section.

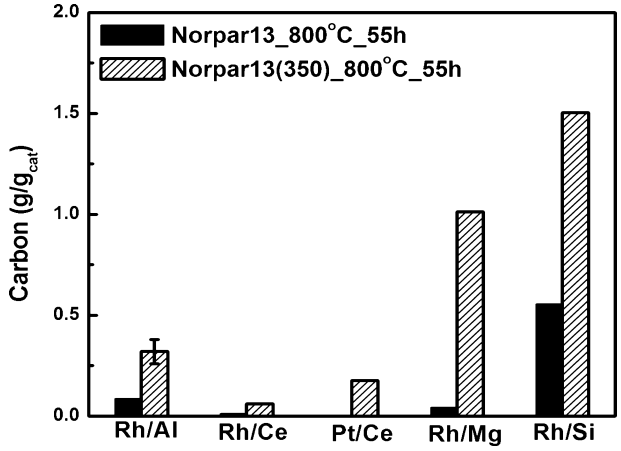

Figure 8. Amounts of carbon deposits in the used Rh catalysts supported on Al_2O_3, CeO_2, SiO_2, and MgO after steam reforming of Norpar13 and Norpar13 doped with 350 ppmw sulfur (Norpar13(350)) as well as that in the Pt/CeO_2 catalyst after steam reforming of Norpar13(350) at 800 °C after 55 h on stream.

lower than those for the Rh catalysts on Al_2O_3, MgO, and SiO_2 and the Pt/Al_2O_3 catalyst after the reaction with sulfur. This difference clearly indicates that CeO_2 as a support is greatly beneficial for reducing the carbon deposition on reforming catalysts, which is also in good agreement with previous studies.[23,51] Figure 9 exhibits the sulfur contents in the used Rh catalysts on the different supports and the used Pt/CeO_2 catalyst after Norpar13(350) reforming for 55 h. In parallel with what we have observed with the Al_2O_3-supported noble metal catalysts, the sulfur content in Rh/Al_2O_3 is apparently higher than those in the other catalysts (Rh/CeO_2, Rh/MgO, and Rh/SiO_2) after Norpar13(350) reforming.

Figure 10 presents the TEM and *Z*-contrast (STEM) images of the used Rh catalysts supported on CeO_2, SiO_2, and MgO as well as Pt/CeO_2 after Norpar13(350) reforming for 55 h. Rh particles in a range of 5−15 nm can be easily identified on these

dx.doi.org/10.1021/cs200695t | *ACS Catal.* 2012, 2, 1127−1137

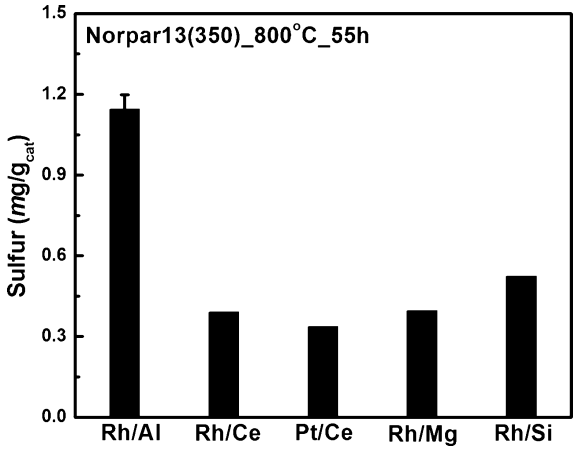

Figure 9. Sulfur contents in the used Rh catalysts supported on Al_2O_3, CeO_2, SiO_2, and MgO as well as that in the Pt/CeO_2 catalyst after steam reforming of Norpar13 doped with 350 ppmw sulfur (Norpar13(350)) at 800 °C after 55 h on stream.

supports, which is significantly larger than those of Rh/Al_2O_3 (1−3 nm). The formation of large Rh particles on CeO_2, SiO_2, and MgO has been widely reported in the literature.[34,52,53] For example, Hennings and Reimert observed that the metal particle sizes of Rh/CeO_2 after steam reforming of natural gas at 800 °C were around 10 nm.[34] Sadi et al. studied the morphological changes of Rh/SiO_2 in a reducing atmosphere and showed that the Rh particles on SiO_2 were largely in a range of 30−40 nm.[52] The much larger Rh particles on SiO_2 can be explained by weak interaction between Rh and SiO_2 such that Rh atoms tend to agglomerate more to form larger particles. Accordingly, it can be inferred that Al_2O_3 is such a support that can effectively stabilize Rh to attain smaller particle sizes in comparison with the other supports investigated in this study.

Sulfur K-edge XANES spectra of the used Rh catalysts after Norpar13(350) reforming for 55 h are shown in Figure 11. Again, the peaks of the oxidized sulfur species (sulfonate and sulfate) for Rh/Al_2O_3 are much stronger than those of the other Rh catalysts. In addition, both Rh/MgO and Rh/SiO_2 exhibit an intensive peak of organic sulfides, which is not the case for Rh/Al_2O_3 and Rh/CeO_2. The peak intensities of metal sulfide, sulfonate, and sulfate are weak for the Rh/MgO and Rh/SiO_2 catalysts due very likely to the severe carbon deposition on these two catalysts upon Norpar13(350) reforming.

4. DISCUSSION

Both the reforming reaction data and the characterization results presented in this work shed light on the pronounced effects of the type of metal and support on the sulfur tolerance and carbon resistance of supported noble metal catalysts in steam reforming of sulfur-containing liquid hydrocarbons. Among the Al_2O_3-supported noble metal catalysts tested, Rh/Al_2O_3 exhibited the best sulfur tolerance under the reforming conditions used in this study. As to the different supports, Al_2O_3 and CeO_2 are the promising ones for Rh catalyst to process hydrocarbons in the presence of sulfur. For the Pt catalyst, Pt/CeO_2 showed better performance than Pt/Al_2O_3 in the reaction with sulfur.

4.1. Stronger Sulfur Tolerance of Rh/Al_2O_3 Compared with Al_2O_3-Supported Ru, Pt, and Pd. As listed in Table 1, the results of H_2 chemisorption and TEM characterization showed that Rh/Al_2O_3 has the highest metal dispersion among the Al_2O_3-supported noble metal catalysts. This is very likely due to the intimate interaction between Rh and Al_2O_3, which is a well-known phenomenon for Al_2O_3-supported Rh catalysts.[41−44,50] The mechanism for the strong interaction between Rh and Al_2O_3 remains unclear, and various hypotheses have been proposed, including (I) the generation of a spinel rhodium-alumina structure through diffusion of Rh into Al_2O_3 bulk,[50] (II) covering Rh by a layer of Al_2O_3,[43] and (III) formation of nonstoichiometric rhodium oxides (e.g., RhO_x) that are capable of strongly interacting with Al_2O_3.[44] Because of the highest metal dispersion, the number of metal sites in Rh/Al_2O_3 available for sulfur adsorption is expected to be higher than those in the other Al_2O_3-supported noble metal catalysts. This is one of plausible reasons that explain the strong sulfur tolerance of Rh/Al_2O_3 in Norpar13(350) reforming at 800 °C.

Sulfur poisoning of supported metal catalysts can be attributed to the strong chemisorptive sulfur adsorption on metals, through which sulfur withdraws electrons from metals and decreases the density of states (DOS) around their Fermi levels.[3,20,21,54] The extent of such an adverse electronic effect of sulfur on metals strongly depends on the nature of the latter. Previous studies[54−56] have pointed out that the tendency of Rh to lose its electrons upon sulfur adsorption is lower than most transition metals.[54−56] For example, recent work has demonstrated that sulfur is able to incur a reduction of about 25% in the DOS near the Fermi level of Rh, whereas that for Pt and Pd is much more significant (ca. 50−55%).[55,56] Therefore, it is also reasonable to relate the strong sulfur tolerance of Rh/Al_2O_3 with the strong resistance of Rh to the sulfur-induced electron withdrawal.

Sulfur K-edge XANES spectra of the used noble metal catalysts (Figure 5) indicate that the formation of sulfonate and sulfate prevailed on Rh/Al_2O_3. It has been proposed that sulfonate and sulfate are less poisoning than metal sulfide because their oxygen-shielded sulfur structure can hinder direct sulfur−metal interactions, thus reducing the poisoning effect of sulfur on metals.[3,20,21] Besides, previous studies regarding sulfur poisoning of supported metal catalysts have indicated that oxidized sulfur species on metals are unstable and tend to migrate onto supports.[57−60] This implies that the Al_2O_3 support in Rh/Al_2O_3 may act as a sulfur trap to accommodate the oxidized sulfur species and then protect Rh from sulfur poisoning. The possible sulfur migration from Rh metals onto the Al_2O_3 support and the sulfur accumulation on the latter may explain the observation that Rh/Al_2O_3 exhibits better catalytic performance than the other catalysts in Norpar13(350) reforming, though it had the highest sulfur content among all the used catalysts.

4.2. Influence of Support on the Catalytic Performance of Rh and Pt. With respect to the effect of support on the sulfur tolerance of supported metal catalysts, there is a general agreement that those on acidic supports have better sulfur tolerance.[61−67] This is because acidic supports favor the formation of electron-deficient metals as a result of electron transfer from metals to acidic supports.[63−66,68−70] Tang et al. reported that the binding energy of Pd $3d_{5/2}$ for strongly acidic Pd/Beta-H (335.5 eV) is higher than that for weaker acidic Pd/Al-MCM-41 (335.0 eV), which supports the formation of electron-deficient metals on acidic supports.[65] Furthermore, Miller et al. compared the sulfur adsorption on Pt catalysts supported on acidic and alkaline zeolites. They claimed that the ratio of S to Pt is lower for the one on the acidic zeolite, indicative of suppressed sulfur adsorption on electron-deficient metals.[63] This is probably because of the difficulty to withdraw electrons from electron-deficient metals by sulfur, thus weakening the interaction between sulfur and metals.[61,63,68] Moreover, it has been suggested that smaller metal particles generally have better sulfur tolerance as metals become electron-deficient when

dx.doi.org/10.1021/cs200695t | ACS Catal. 2012, 2, 1127−1137

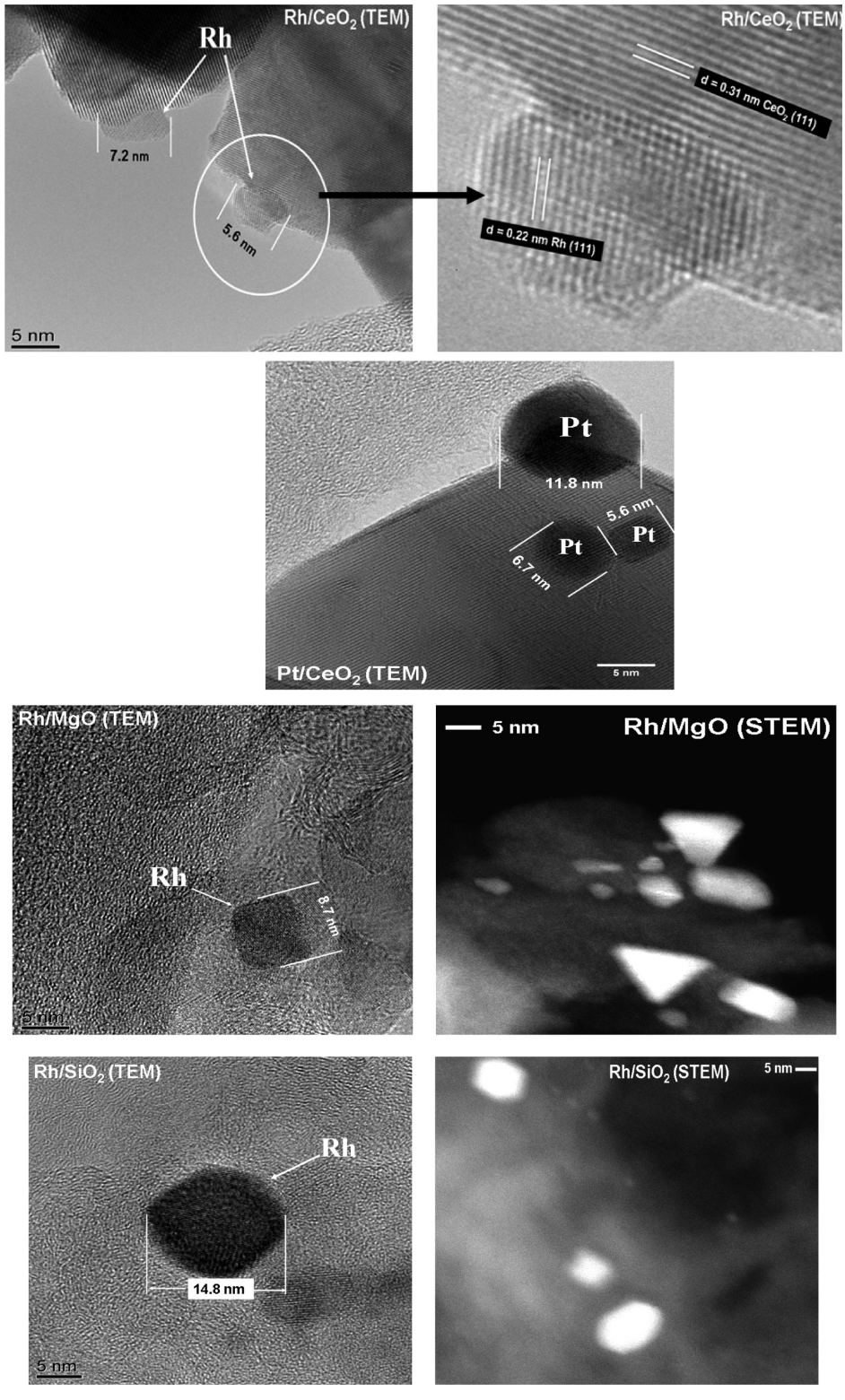

Figure 10. High-resolution TEM and *Z*-contrast (STEM) images of the used Rh catalysts supported on CeO_2, SiO_2, and MgO as well as a TEM image of the Pt/CeO_2 catalyst after steam reforming of Norpar13 doped with 350 ppmw sulfur (Norpar13(350)) at 800 °C after 55 h on stream. The brighter spots in the *Z*-contrast (STEM) images represent metal particles. For Rh/CeO_2, *d*-space analysis confirms a Rh particle supported on CeO_2. The white lines in the TEM images were used to help locate the noble metal particles and measure their sizes.

their particle sizes decrease.[71−73] Sheu et al.[73] investigated the sulfur tolerance of Pd catalysts loaded on SiO_2, TiO_2, and TiO_2-grafted SiO_2 in tetralin hydrogenation. The authors claimed that the Pd catalyst on TiO_2-grafted SiO_2 was the most sulfur tolerant, which was ascribed to the retardation effect of TiO_2 modification on the growth of Pd crystallites, resulting in the formation of electron-deficient Pd particles.

The superior sulfur tolerance of Rh/Al_2O_3 in Norpar13(350) reforming may be related to the smaller Rh particles and the acidic Al_2O_3 support, both of which may aid in the formation of

dx.doi.org/10.1021/cs200695t | *ACS Catal.* 2012, 2, 1127−1137

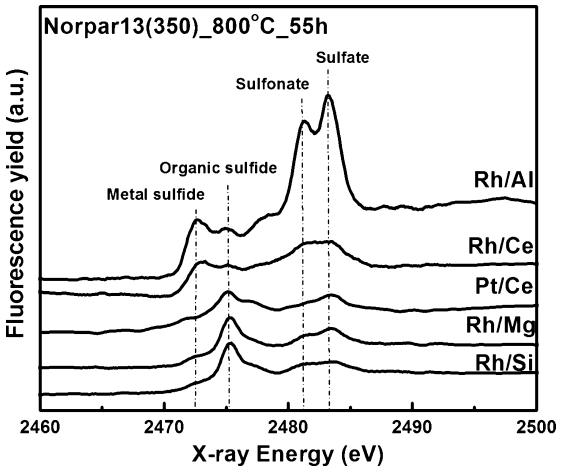

Figure 11. Sulfur K-edge XANES spectra of the used Rh catalysts supported on Al_2O_3, CeO_2, SiO_2, and MgO as well as the Pt/CeO_2 catalyst after steam reforming of Norpar13 doped with 350 ppmw sulfur (Norpar13(350)) at 800 °C after 55 h on stream.

electron-deficient Rh particles with improved sulfur tolerance. To confirm this hypothesis, XPS was carried out to measure the binding energy (B.E.) of the fresh Rh catalysts supported on Al_2O_3 and CeO_2. As shown in Figure 12, The B.E. for the unreduced and reduced Rh/CeO_2 catalysts is 309.0 (Rh^{3+}) and 307.0 (Rh^0) eV, respectively.[37] Remarkable B.E. shifts to higher energy were observed for the unreduced (309.8 eV) and reduced (307.6 eV) Rh/Al_2O_3 catalysts compared with the Rh/CeO_2 catalyst and Rh standards (see Table 2). These XPS results strongly suggest the formation of electron-deficient Rh particles on the Al_2O_3 support as compared to those on CeO_2. Because of the weaker interaction between sulfur and electron-deficient metals,[54,63,68] the bonding between the adsorbed sulfur and the Rh particles in Rh/Al_2O_3 may be readily broken, followed by sulfur oxidation induced by the surface oxygen species derived from steam activation in the reforming reaction. This may account for the preferential oxidation of sulfur on the Rh/Al_2O_3 catalysts after the reaction with sulfur.

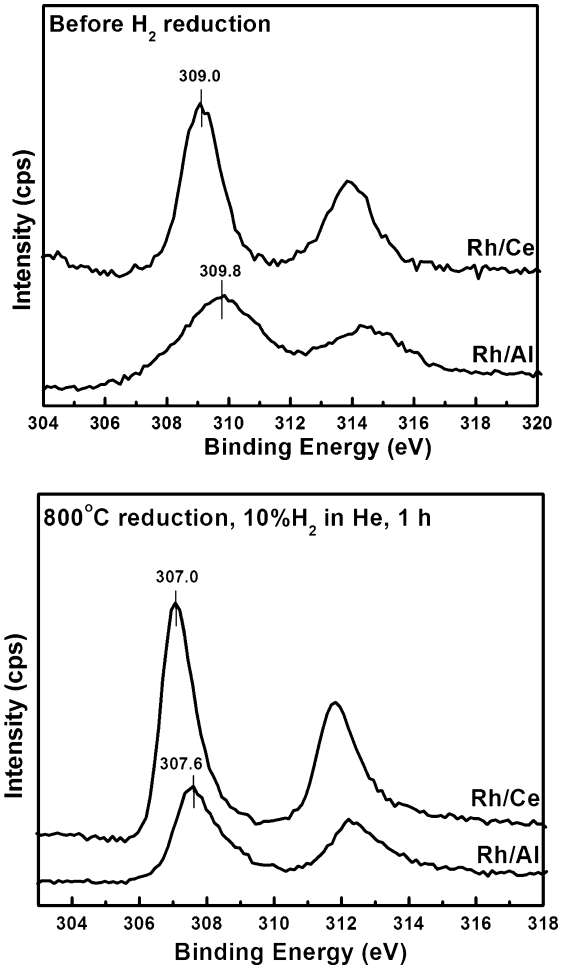

Figure 12. Rh 3d XPS spectra of the unreduced and reduced (800 °C) Rh catalysts supported on Al_2O_3 and CeO_2.

Table 2. Rh 3d XPS Data of Unreduced and Reduced Rh/Al_2O_3 and Rh/CeO_2

samples	pretreatment	Rh $3d_{5/2}$ (eV)	fwhm	Rh $3d_{3/2}$ (eV)	fwhm	ΔE (eV)[a]
Rh/Al_2O_3	unreduced	309.8	2.8	314.6	2.7	4.8
	reduced	307.6	1.5	312.3	1.8	4.7
Rh/CeO_2	unreduced	309.0	1.4	313.9	1.8	4.8
	reduced	307.0	1.1	311.8	1.4	4.8
Rh metal[c]	used as rec'd	307.0	N/A[b]	312.0	N/A[b]	5.0
Rh_2O_3[c]	used as rec'd	308.8	N/A[b]	313.6	N/A[b]	4.8

[a]Spin−orbit coupling energy. [b]Not available. [c]Reference 37.

It is very interesting to note that, although CeO_2 is not an acidic support and the Rh particles on Rh/CeO_2 are larger than those on Rh/Al_2O_3, the two catalysts showed very similar catalytic performance in Norpar13(350) reforming. This can be attributed to the strong oxygen storage capability of CeO_2 that enables the facile release of its surface oxygen species to facilitate carbon gasification.[14,15,39,49,51] Therefore, the amounts of carbon deposits on the used Rh/CeO_2 catalysts upon Norpar13 reforming without and with sulfur are much lower compared with those supported on Al_2O_3, SiO_2, and MgO (Figure 8). The promotion effect of CeO_2 on carbon gasification may also account for the much lower carbon deposition on Pt/CeO_2 than that on Pt/Al_2O_3 as well as the better catalytic performance of the former in the sulfur-containing reaction.

5. CONCLUSIONS

The present study demonstrated the pronounced influence of the type of metal and support on the sulfur tolerance and carbon resistance of supported noble metal catalysts in steam reforming of sulfur-containing liquid hydrocarbons at 800 °C with a steam/carbon molar ratio of 3 for 55 h. Under the reforming conditions used in this work, the Rh/Al_2O_3 catalyst showed better sulfur tolerance than the Ru, Pt, and Pd catalysts on the same support. Moreover, both Al_2O_3 and CeO_2 were proven to be promising supports for the Rh catalyst to process liquid hydrocarbons in the presence of sulfur. As to the Pt catalyst, CeO_2 was found to be a better support than Al_2O_3 in the reforming reaction with sulfur.

The strong sulfur tolerance of Rh/Al_2O_3 can be explained by the formation of well-dispersed electron-deficient Rh particles, as revealed by H_2-chemisorption, TEM, and XPS. The well-dispersed Rh particles imply that the Rh/Al_2O_3 catalyst possesses more metal surface sites than the other catalysts toward sulfur adsorption. Sulfur K-edge XANES indicated that the formation of sulfonate and sulfate predominated on the used Rh/Al_2O_3 catalyst after the reaction with sulfur. It is

dx.doi.org/10.1021/cs200695t | ACS Catal. 2012, 2, 1127−1137

proposed that the electron-deficient characteristic of the Rh particles on Al_2O_3 may weaken Rh−S bonds, thus favoring the sulfur oxidation on the Rh/Al_2O_3 catalyst. The oxygen-shielded sulfur structure of sulfonate and sulfate may hinder direct Rh−S interaction and suppress the poisoning effect of adsorbed sulfur species on the Rh/Al_2O_3 catalyst. Because of the better sulfur tolerance of Rh/Al_2O_3, the carbon deposition on this catalyst was much lower than that on the Al_2O_3-supported Ru, Pt, and Pd catalysts upon Norpar13(350) reforming.

The superior catalytic performance of the CeO_2-supported Rh and Pt catalysts in the reaction with sulfur can be ascribed mainly to the promotion effect of CeO_2 on carbon gasification, leading to the much lower carbon deposition compared with the Rh/Al_2O_3, Rh/MgO, Rh/SiO_2, and Pt/Al_2O_3 catalysts in the presence of sulfur.

AUTHOR INFORMATION

Corresponding Author

*E-mail: csong@psu.edu. Phone: 814-863-4466. Fax: 814-865-3573.

Funding

This work was supported in part by U.S. Department of Energy National Energy Technology Laboratory under Grant DE-NT0004396 and by U.S. Office of Naval Research through an ONR NAVSEA Grant N00014-06-1-0320. Sulfur XANES work at the CMC Beamline is supported in part by the Office of Basic Energy Sciences of the U.S. Department of Energy and by the National Science Foundation Division of Materials Research. Use of the Advanced Photon Source is supported by the Office of Basic Energy Sciences of the U.S. Department of Energy under Contract No. W-31-109-Eng-38. The Environmental Molecular Sciences Laboratory (EMSL), a national scientific user facility at Pacific Northwest National Laboratory (PNNL), Richland, WA, is gratefully acknowledged for XPS measurements under general user proposal 37791.

Notes

The authors declare no competing financial interest.

REFERENCES

(1) Song, C. S. *Catal. Today* **2002**, *77*, 17−49.
(2) Trimm, D. L. *Appl. Catal.* **1983**, *5*, 263−290.
(3) Bartholomew, C. H. *Appl. Catal., A* **2001**, *212*, 17−60.
(4) Bartholomew, C. H. *Catal. Rev. - Sci. Eng.* **1982**, *24*, 67−112.
(5) Trimm, D. L. *Catal. Rev. - Sci. Eng.* **1977**, *16*, 155−189.
(6) Trimm, D. L. *Catal. Today* **1997**, *37*, 233−238.
(7) Trimm, D. L. *Catal. Today* **1998**, *49*, 3−10.
(8) Sehested, J. *Catal. Today* **2006**, *111*, 103−110.
(9) Nikolla, E.; Schwank, J. W.; Linic, S. *Catal. Today* **2007**, *136*, 243−248.
(10) Nikolla, E.; Schwank, J.; Linic, S. *J. Catal.* **2007**, *250*, 85−93.
(11) Nikolla, E.; Schwank, J.; Linic, S. *J. Catal.* **2009**, *263*, 220−227.
(12) Nikolla, E.; Holewinski, A.; Schwank, J.; Linic, S. *J. Am. Chem. Soc.* **2006**, *128*, 11354−11355.
(13) Nikolla, E.; Schwank, J.; Linic, S. *J. Am. Chem. Soc.* **2009**, *131*, 2747−2754.
(14) Natesakhawat, S.; Watson, R. B.; Wang, X. Q.; Ozkan, U. S. *J. Catal.* **2005**, *234*, 496−508.
(15) Song, H.; Ozkan, U. S. *J. Catal.* **2009**, *261*, 66−74.
(16) Bengaard, H. S.; Norskov, J. K.; Sehested, J.; Clausen, B. S.; Nielsen, L. P.; Molenbroek, A. M.; Rostrup-Nielsen, J. R. *J. Catal.* **2002**, *209*, 365−384.
(17) Rostrup-Nielsen, J. R. *J. Catal.* **1974**, *33*, 184−201.
(18) Helveg, S.; Lopez-Cartes, C.; Sehested, J.; Hansen, P. L.; Clausen, B. S.; Rostrup-Nielsen, J. R.; Abild-Pedersen, F.; Norskov, J. K. *Nature* **2004**, *427*, 426−429.
(19) Rostrup-Nielsen, J. R.; Sehested, J.; Norskov, J. K. *Adv. Catal.* **2002**, *47*, 65−139.
(20) Bartholomew, C. H.; Agrawal, P. K.; Katzer, J. R. *Adv. Catal.* **1982**, *31*, 135−242.
(21) Maxted, E. B. *Adv. Catal.* **1951**, *3*, 129−178.
(22) Chen, Y. S.; Xie, C.; Li, Y.; Song, C. S.; Bolin, T. *Phys. Chem. Chem. Phys.* **2010**, *12*, 5707−5711.
(23) Strohm, J. J.; Zheng, J.; Song, C. S. *J. Catal.* **2006**, *238*, 309−320.
(24) Ferrandon, M.; Krause, T. *Appl. Catal., A* **2006**, *311*, 135−145.
(25) Ferrandon, M.; Mawdsley, J.; Krause, T. *Appl. Catal., A* **2008**, *342*, 69−77.
(26) Shekhawat, D.; Gardner, T. H.; Berry, D. A.; Salazar, M.; Haynes, D. J.; Spivey, J. J. *Appl. Catal., A* **2006**, *311*, 8−16.
(27) Kaila, R. K.; Gutierrez, A.; Slioor, R.; Kemell, M.; Leskela, M.; Krause, A. O. I. *Appl. Catal., B* **2008**, *84*, 223−232.
(28) Xue, Q. S.; Gao, L.; Lu, Y. *Catal. Today* **2008**, *146*, 103−109.
(29) Lu, Y.; Chen, J. C.; Liu, Y.; Xue, Q. S.; He, M. Y. *J. Catal.* **2008**, *254*, 39−48.
(30) Xie, C.; Chen, Y. S.; Li, Y.; Wang, X. X.; Song, C. S. *Appl. Catal. A: Gen.* **2010**, *390*, 210−218.
(31) Xie, C.; Chen, Y.; Li, Y.; Wang, X.; Song, C. *Appl. Catal., A* **2011**, *394*, 32−40.
(32) Azad, A. M.; Duran, M. J. *Appl. Catal., A* **2007**, *330*, 77−88.
(33) Azad, A. M.; Duran, M. J.; McCoy, A. K.; Abraham, M. A. *Appl. Catal., A* **2007**, *332*, 225−236.
(34) Hennings, U.; Reimert, R. *Appl. Catal., B* **2005**, *70*, 498−508.
(35) Bernal, S.; Botana, F. J.; Calvino, J. J.; Cifredo, G. A.; Perez-Omil, J. A.; Pintado, J. M. *Catal. Today* **1995**, *23*, 219−250.
(36) Bernal, S.; Calvino, J. J.; Cauqui, M. A.; Gatica, J. M.; Larese, C.; Pez Omil, J. A.; Pintado, J. M. *Catal. Today* **1999**, *50*, 175−206.
(37) Kugai, J.; Subramani, V.; Song, C. S.; Engelhard, M. H.; Chin, Y.-H. *J. Catal.* **2006**, *238*, 430−440.
(38) El Fallah, J.; Boujana, S.; Dexpert, H.; Kiennemann, A.; Majerus, J.; Touret, O.; Villain, F.; Le Normand, F. *J. Phys. Chem.* **1994**, *98*, 5522−5533.
(39) Li, Y.; Wang, X. X.; Xie, C.; Song, C. S. *Appl. Catal., A* **2009**, *357*, 213−222.
(40) Ravel, B.; Newville, M. *J. Synch. Rad.* **2005**, *12*, 537−541.
(41) Vantblik, H. F. J.; Vanzon, J.; Huizinga, T.; Vis, J. C.; Koningsberger, D. C.; Prins, R. *J. Am. Chem. Soc.* **1985**, *107*, 3139−3147.
(42) Koningsberger, D. C.; Vanzon, J.; Vantblik, H. F. J.; Visser, G. J.; Prins, R.; Mansour, A. N.; Sayers, D. E.; Short, D. R.; Katzer, J. R. *J. Phys. Chem.* **1985**, *89*, 4075−4081.
(43) Chen, J. G.; Colaianni, M. L.; Chen, P. J. J.; Yates, J. T.; Fisher, G. B. *J. Phys. Chem.* **1990**, *94*, 5059−5062.
(44) Beck, D. D.; Capehart, T. W.; Wong, C.; Belton, D. N. *J. Catal.* **1993**, *144*, 311−324.
(45) Zhao, Y. J.; Zhou, J.; Zhang, J. G.; Wang, S. D. *Catal. Lett.* **2009**, *131*, 597−605.
(46) Nagai, Y.; Hirabayashi, T.; Dohmae, K.; Takagi, N.; Minami, T.; Shinjoh, H.; Matsumoto, S. *J. Catal.* **2006**, *242*, 103−109.
(47) George, G. N.; Gorbaty, M. L. *J. Am. Chem. Soc.* **1989**, *111*, 3182−3186.
(48) Ota, H.; Akai, T.; Namita, H.; Yamaguchi, S.; Nomura, M. *J. Power Sources* **2003**, *119*, 567−571.
(49) Trovarelli, A. *Catal. Rev. - Sci. Eng.* **1996**, *38*, 439−520.
(50) Yao, H. C.; Japar, S.; Shelef, M. *J. Catal.* **1977**, *50*, 407−418.
(51) Wang, S. B.; Lu, G. Q. *Appl. Catal., B* **1998**, *19*, 267−277.
(52) Sadi, F.; Duprez, D.; Gerard, F.; Rossignol, S.; Miloudi, A. *Catal. Lett.* **1997**, *44*, 221−228.
(53) Tanaka, H.; Kaino, R.; Okumura, K.; Kizuka, T.; Tomishige, K. *J. Catal.* **2009**, *268*, 1−8.
(54) Rodriguez, J. A.; Hrbek, J. *Acc. Chem. Res.* **1999**, *32*, 719−728.
(55) Rodriguez, J. A.; Kuhn, M.; Hrbek, J. *Chem. Phys. Lett.* **1996**, *251*, 13−19.
(56) Rodriguez, J. A.; Chaturvedi, S.; Jirsak, T. *Chem. Phys. Lett.* **1998**, *296*, 421−428.

(57) Gracia, F. J.; Guerrero, S.; Wolf, E. E.; Miller, J. T.; Kropf, A. *J. Catal.* **2005**, *233*, 372−387.
(58) Wakita, H.; Kani, Y.; Ukai, K.; Tomizawa, T.; Takeguchi, T.; Ueda, W. *Appl. Catal., A* **2005**, *283*, 53−61.
(59) Shimizu, K.; Higashimata, T.; Tsuzuki, M.; Satsuma, A. *J. Catal.* **2006**, *239*, 117−124.
(60) Wu, Q.; Gao, H. W.; He, H. *J. Phys. Chem. B* **2006**, *110*, 8320−8324.
(61) Corma, A.; Martinez, A.; Martinez-Soria, V. *J. Catal.* **1997**, *169*, 480−489.
(62) Niquille-Rothlisberger, A.; Prins, R. *Catal. Today* **2007**, *123*, 198−207.
(63) Miller, J. T.; Koningsberger, D. C. *J. Catal.* **1996**, *162*, 209−219.
(64) Tang, T.; Yin, C.; Wang, L.; Ji, Y.; Xiao, F. S. *J. Catal.* **2007**, *249*, 111−115.
(65) Tang, T.; Yin, C.; Wang, L.; Ji, Y.; Xiao, F. S. *J. Catal.* **2008**, *257*, 125−133.
(66) Yasuda, H.; Matsubayashi, N.; Sato, T.; Yoshimura, Y. *Catal. Lett.* **1998**, *54*, 23−27.
(67) Yasuda, H.; Sato, T.; Yoshimura, Y. *Catal. Today* **1999**, *50*, 63−71.
(68) Frety, R.; Dasilva, P. N.; Guenin, M. *Catal. Lett.* **1989**, *3*, 9−16.
(69) Sachtler, W. M. H.; Stakheev, A. Y. *Catal. Today* **1992**, *12*, 283−295.
(70) Simon, L. J.; van Ommen, J. G.; Jentys, A.; Lercher, J. A. *J. Catal.* **2001**, *201*, 60−69.
(71) Matsui, T.; Harada, M.; Ichihashi, Y.; Bando, K. K.; Matsubayashi, N.; Toba, M.; Yoshimura, Y. *Appl. Catal., A* **2005**, *286*, 249−257.
(72) Ryndin, Y. A.; Stenin, M. V.; Boronin, A. I.; Bukhtiyarov, V. I.; Zaikovskii, V. I. *Appl. Catal.* **1989**, *54*, 277−288.
(73) Sheu, H. S.; Lee, J. F.; Shyu, S. G.; Chou, W. W.; Chang, J. R. *J. Catal.* **2009**, *266*, 15−25.